Available online www.jocpr.com

Journal of Chemical and Pharmaceutical Research, 2016, 8(3):807-822

Research Article

ISSN : 0975-7384
CODEN(USA) : JCPRC5

Design, synthesis and molecular docking studies of azido-pyrimidine analogues as anti-bacterial and anti-fungal agents

Nitin K. Longadge[1]*, Anjali M. Rahatgaonkar[2] and Binda. D. Saraf[1]

[1]*Department of Chemistry, Institute of Science, Nagpur, Maharashtra, India*
[2]*Department of Forensic Chemistry and Toxicology, Institute of Forensic Science, Nagpur, Maharashtra, India*

ABSTRACT

As part of our exploration for new antibacterial and antifungal agents, a series of 2-(2-amino-5-azido-6-phenylpyrimidin-4-yl)-4-substituted phenols hybrids were synthesized. Simulation of virtually designed 25 compounds have been studied for their binding active sites of tyrosyl-tRNA synthetase (TyrRS) and cytochrome P450 14□-sterol demethylase CPY51 enzyme using molecular modeling of protein– ligand interactions to predict drug structure–activity relationship. For comparison, the binding behavior of known standard drugs has also been studied. Synthesized compounds were screened for their in vitro antibacterial activity against Staphylococcus aureus, Salmonella typhi, antifungal activity against the opportunistic pathogens Candida albicans and Aspergillus niger. The objective of our research is to accept the challenge of discovery of new drug. To ensure the desired target specificity and potency, bioavailability and lack of toxicity, our approach stems out lead generation from virtual screening to their synthesis and ends up with biological assays.

Key words: Azidopyrimidines, Ionic liquid, Docking, tyrosyl-tRNA synthetase (TyrRS), cytochrome P450, Antimicrobial activity.

INTRODUCTION

There is a growing demand for the preparation of new antimicrobial agents due to the developing resistance towards conventional antibiotics [1]. The development of resistance to clinically used drugs has encouraged development of novel antimicrobial agents which selectively constrain novel bacterial and fungal targets [2-4]. In this regard, aminoacyl-tRNA synthetases (aaRSs) have attracted considerable interest in antibacterial drug discovery. It is well known that aaRSs are responsible for faithful translation of nucleic acid sequence information into proteins [5-6]. Consequently, once these enzymes are inhibited, cell growth is inhibited due to protein biosynthesis being halted. Nevertheless, the topology of the ATP binding domain and the functions of the human aaRSs differ from those of bacteria, thus providing an opportunity to inhibit them selectively in bacteria [7-8]. These enzymes, therefore, are attractive targets (**Fig. 1**) for antibacterial agents [9].

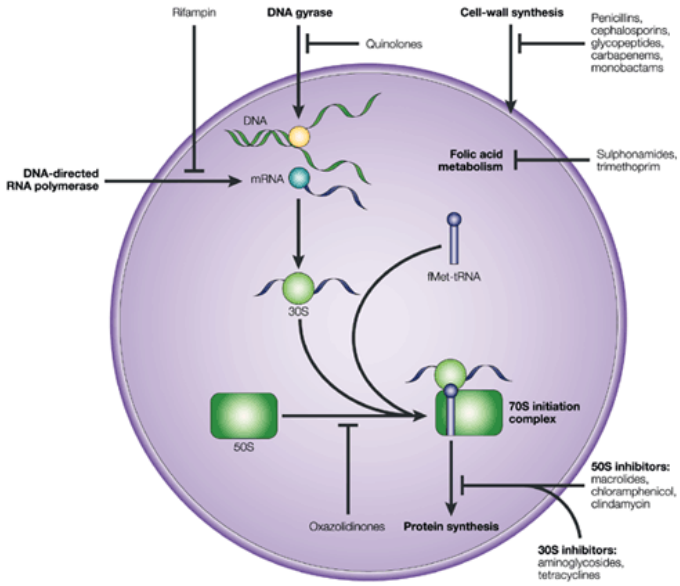

Figure 1 Targets for antibacterial therapy [10]

Fungal infections cause a continuous and momentous threat to human health, especially in immune-compromised patients.1,2 Drug resistance among fungal pathogens is an increasing problem, thus it is requisite to develop some novel antifungal compounds with high efficacy, less toxicity and low resistance [11].

Ergosterol is the major component of the fungal cell membrane. It is as a bio-regulator of membrane fluidity, asymmetry and integrity. Inhibition of the 14α-demethylase will result in a decreased ergosterol synthesis and a concomitant accumulation of 14-methylated sterols. They prevent the 14-α demethylation of lanosterol into ergosterol in the ergosterol synthetic pathway [12-13]. Thereby preventing the post-squalene synthesis segments such as the oxidosqualene cyclase methyltransferase [14]. Ergosterol plays a hormone- like role in fungal cells, which stimulates growth; the net effect of synthesized molecules is the inhibition the fungal growth (**Fig. 2**).

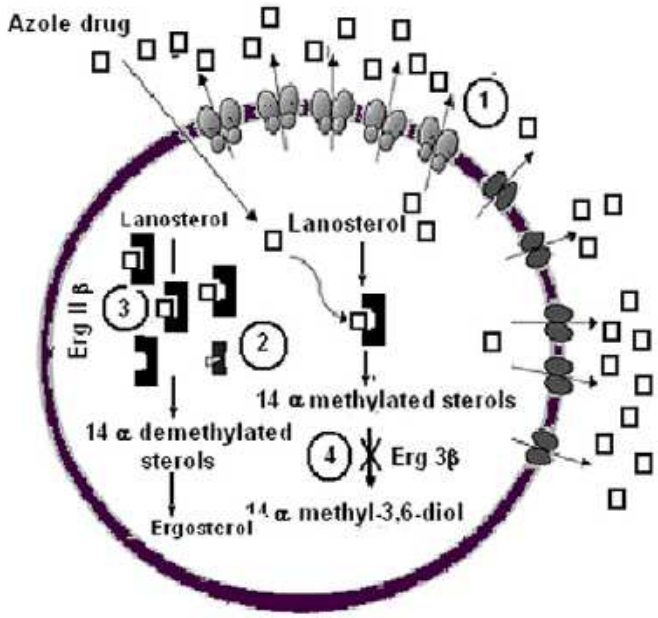

Figure 2 Mechanism of azoles drugs in biosynthesis pathway [15]

Most of the nitrogen-containing molecules are pharmacologically very active which can be attributed to the fact that nitrogenous compounds are part and parcel of the biomolecular diversity [16]. Azides are considered to be very important class of compounds due to their both industrial as well as biological applications. The chemistry of azides thus attracted the attention of many chemists since many of these compounds play important role in organic chemistry [17]. Amongst the pharmacologically active nitrogenous compounds, a large number of Azido-Pyrimidine and their derivatives attracted considerable attention for the past few decades due to their chemotherapeutical value. Azido-Pyrimidine framework is a part of many synthetic compounds, which possess useful biological activities including Antiviral and antineoplastic activities [18], Anti-inflammatory Activity [19], anti-tumor [20], dihydrofolate reductase inhibitors [21], antiviral activity against hepatitis-A virus (HAV) and herpes simplex virus type-1 (HSV-1) [22], Inhibitors of AP-1 and NF-κB Mediated Gene Expression [23], Therefore, azido derivatives of pyrimidine have been receiving significant attention. Recent studies reported pyrimidine derivatives showing good antibacterial and antifungal activity [24-26] which encourages us to synthesize and evaluate the antibacterial and antifungal activity of a series of 2-(2-amino-5-azido-6-phenylpyrimidin-4-yl)-4-substituted phenols.

In our work for finding new antibacterial agents, we have explored a series of 2-(2-amino-5-azido-6-phenylpyrimidin-4-yl)-4-substituted phenols as potent inhibitors against tyrosyl-tRNA synthetase (TyrRS) [27], one of the aminoacyl-tRNA synthetases (aaRSs) and for finding new antifungal agents, against lanosterol 14 □-sterol demethylase which block ergosterol synthesis by interfering with the demethylation of its precursor [15].

Recently, ionic liquid (IL) have attracted much attention towards academic and industrial research since they have shown intense advantages in the context of green chemistry and therefore have great promising potential. Ionic materials are used as a substitute for volatile solvents in organic synthesis. This class of solvent often combines attractive features of considerable thermal stability and low vapor pressure in a single solvent system. ILs are mainly composed of symmetrical and of bulky organic cation paired with anion that can be either organic or inorganic in nature. Moreover, it is well known that physical and chemical properties of an IL are determined by structure of constituent cation and anion. Thus one can systematically tailor an IL with specific properties. Ionic liquids (ILs) are molten salts with melting points below 100^0C [28]. The hydrophobic ionic liquid [bmim][PF_6] is well known for its capability in various catalytic applications. In particular, hydrophobic media possessing hexafluorophosphate anions have a multitude of uses in different biochemical and chemical reactions [29].

Herein, we have investigated the effect of different reaction conditions involving model hydrophobic ionic liquids, such as [bmim][PF_6], on the formation of 2-(2-amino-5-azido-6-phenylpyrimidin-4-yl)-4-substituted phenols, and we illustrate herein the extension of the use of [bmim][PF_6] to reactions of diversely substituted substrates.

To the best of our knowledge, there has been no previous report of analogous pyrimidines as antibacterial and antifungal agents. However, there are numerous examples of nitrogen containing heterocycles being used to treat microbial infections; these compounds may lead to the generation of novel anti-microbial therapeutics.

The combination of genomics and bioinformatics has the potential to generate the information and knowledge that will enable the conception and development of new therapies and interventions needed to treat and to elucidate the unusual biology of these microbial infections. One of the most important applications of molecular modeling techniques in structural biology is docking of a ligand molecule to a receptor, such as a protein. In pursuit of achieving this goal, our research efforts led to the development of hybrid molecule of pyrimidines and azides as novel and diversely substituted scaffolds which can be utilized further as templates for anti-microbial agents.

EXPERIMENTAL SECTION

[bmim][PF_6] was obtained from Acros Organics (New Jersey, USA), all solvents were dried by standard methods. Melting points were determined by open capillary method and are uncorrected. Chemicals were obtained from S.D. Fine of AR Grade Analytical. TLCs were carried out on 0.25-mm layer silica gel plates, and single spots were obtained. Column chromatography was performed with silica gel of 120 mesh (Merk).^{1}H NMR, and ^{13}CNMR spectra were recorded from $CDCl_3$/DMSO-d_6 solution on a Brucker Avance II 400 (400 MHz) NMR Spectrometer. The chemical shifts in ppm are expressed on the δ scale using tetramethylsilane as internal standard. Coupling constants are given in Hz. IR spectra were obtained on a Perkin Elmer 1800 spectrophotometer using KBr discs. Elemental analyses were carried out using Perkin Elmer 2400 elemental analyzer. Mass spectra were measured with a GC–MS (70 eV). The purity of the samples was checked by TLC and spectroscopic data. The X-ray diffraction

patterns have been recorded in 2θ range from 13 to 600 on Philips (Holland) automated X-ray powder diffractometer. The operating target voltage was 35kV and tube current was 20mA. The scanning speed was 0.5 2θ/min. Radiation used was *Cu-k* of wavelength 1.54056 Å provided with a monochromator for filtering β radiations to reduce noise due to white radiations and to increase the resolution. The values of inter-planer spacing (d) corresponding to Bragg reflections (2θ) were obtained. Indexing and calculations of unit cell parameters were performed with the help of Powder-X-Software [30].

General synthetic procedure for 2-(2-amino-5-azido-6-phenylpyrimidin-4-yl)-4-methylphenol (2a)
The synthetic route was achieved through ionic liquid [bmim][PF_6] serving as dual solvent and catalyst, leading to quick, easy and enhanced yield. This rational chemical approach afforded azido derivative of pyrimidines.

Substituted azido pyrimidines were synthesized efficiently by cyclization of 3-azido-6-substituted-2-phenyl-4H-chromen-4-one using guanidine carbonate in [bmim][PF_6]. The whole procedure is simple and straightforward. By employing this protocol, a series of novel 2-(2-amino-5-azido-6-phenylpyrimidin-4-yl)-4-substituted phenols hybrids were prepared.

A mixture of 3-azido-6-methyl-2-phenyl-4H-chromen-4-one (1mmol, 0.277 g), guanidine carbonate (2mmol. 0.36 g) and 2 mL of ionic liquid [bmim][PF_6] were added in a round bottom flask in an inert atmosphere and stirred at room temperature for 15minutes and the reaction was monitored by TLC. After completion of reaction, it was cooled and poured in 20 % HCl solution, filtered and washed with water. The solid obtained was recrystallized from ethanol (**Scheme 1**). Yield, 97 % (0.3104g); mp 210 ^{0}C; IR (KBr), υ (cm^{-1}): 3498 (O-H), 3312 (N–H), 2922 (CH_3 str), 2138 (N_3), 1639 (N-H deformation for pri. amine), 1470 (-CH_3 bend), 1380 (-CH_3 bend.), 1395 (C=N str.), 1529 (C=C bend.), ^{1}H NMR ($DMSOd_6$), δ (ppm): 2.3 (s, 3H, -CH_3), 4.6 (s, 2H, -NH_2), 6.91-6.94 (d, 1H, J = 12.2 Hz, Ha), 7.18–7.22 (dd, 1H, J = 2.4, 10.8 Hz, Hb), 7.4-7.5 (m, 5H, Ar-H), 8.1 (s, 1H, Hc), 13.6 (s, 1H, -OH). ^{13}C NMR (200 MHz $DMSOd_6$), δ 20.06, 100.49, 116.63, 117.77, 126.46, 126.59, 127.13, 128.13, 130.05, 133.08, 136.87, 136.99, 158.01, 160.68, 165.13, 165.66. Mass (m/z): 318 M^+; Elemental analysis: Calculated for ($C_{17}H_{14}N_6O$): C 64.14, H 4.43, N 26.40, O 5.03 Found: C 64.55, H 4.25, N 26.08, O 5.12. The series of substituted compounds **2b-l** were synthesized following above procedure.

2-(2-amino-5-azido-6-phenylpyrimidin-4-yl)-4-chlorophenol (2b)
Yield, 95 %; mp 244 ^{0}C; IR (KBr), υ (cm^{-1}): 3500 (O-H), 3310 (N–H), 2926 (CH_3 str), 2120 (N_3), 1640 (N-H deformation for pri. amine), 852 (C-Cl str) 1472 (-CH_3 bend), 1383 (-CH_3 bend.), 1415 (C=N str.), 1530 (C=C bend.), ^{1}H NMR ($CDCl_3$), δ (ppm): 4.7 (s, 2H, -NH_2), 6.5-6.6 (d, 1H, J = 9.48, Ha), 6.71-6.76 (dd, 1H, J = 1.84, 3.52, Hb), 6.9-7.1 (m, 5H, Ar-H), 7.14 (s, 1H, Hc), 10.5 (s, 1H, -OH). ^{13}C NMR (200 MHz $CDCl_3$), δ 98.6, 117.6, 119.2, 126.7, 129.1, 135.7, 136.1, 136.5, 139.8, 152.5, 158.8, 160.2, 166.8 Mass (m/z): 338 M^+; Elemental analysis: Calculated for ($C_{16}H_{11}ClN_6O$): C, 56.73; H, 3.27; Cl, 10.47; N, 24.81; O, 4.72 Found: C, 56.69; H, 3.25; Cl, 10.41; N, 24.85; O, 4.76.

2-(2-amino-5-azido-6-phenylpyrimidin-4-yl)-6-bromo-4-methylphenol (2c)
Yield, 90 %; mp 188 ^{0}C; IR (KBr), υ (cm^{-1}): 3494 (O-H), 3310 (N–H), 2926 (CH_3 str), 2095 (N_3), 1637 (N-H deformation for pri. amine), 1471 (-CH_3 bend), 1382 (-CH_3 bend.), 1396 (C=N str.), 1528 (C=C bend.), ^{1}H NMR ($CDCl_3$), δ (ppm): 2.3 (s, 3H, -CH_3), 5.0 (s, 2H, -NH_2), 7.2-7.5 (m, 5H, Ar-H), 7.5 (s, 1H, Ha), 7.6 (s, 1H, Hb), 10.2 (s, 1H, -OH). ^{13}C NMR (200 MHz $CDCl_3$), δ 22.71, 106.99, 113.91, 126.72, 127.96, 128.07, 128.31, 128.76, 129.02, 132.25, 132.28, 134.35, 135.82, 136.55, 140.64, 158.56, 159.92, 170.32 Mass (m/z): 396 M^+; Elemental analysis: Calculated for ($C_{17}H_{13}BrN_6O$): C, 51.40; H, 3.30; Br, 20.12; N, 21.16; O, 4.03 Found: C, 51.42; H, 3.26; Br, 20.18; N, 21.11; O, 4.07.

2-(2-amino-5-azido-6-phenylpyrimidin-4-yl)-6-bromo-4-chlorophenol (2d)
Yield, 94 %; mp 256 ^{0}C; IR (KBr), υ (cm^{-1}): 3492 (O-H), 3314 (N–H), 2921 (CH_3 str), 2124 (N_3), 1637 (N-H deformation for pri. amine), 1473 (-CH_3 bend), 1382 (-CH_3 bend.), 1397 (C=N str.), 1528 (C=C bend.), ^{1}H NMR ($CDCl_3$), δ (ppm): 4.5 (s, 2H, -NH_2), 7.2-7.9 (m, 5H, Ar-H), 7.6 (s, 1H, Ha), 7.8 (s, 1H, Hb), 10.9 (s, 1H, -OH). ^{13}C NMR (200 MHz $CDCl_3$), δ 99.29, 118.30, 123.83, 124.89, 127.18, 127.76, 128.13, 130.26, 134.15, 152.53, 158.35, 161.40, 164.10 Mass (m/z): 417 M^+; Elemental analysis: Calculated for ($C_{16}H_{10}BrClN_6O$): C, 46.01; H, 2.41; Br, 19.13; Cl, 8.49; N, 20.12; O, 3.83 Found: C, 46.09; H, 2.44; Br, 19.17; Cl, 8.41; N, 20.08; O, 3.78.

2-(2-amino-5-azido-6-phenylpyrimidin-4-yl)-6-iodo-4-methylphenol (2e)
Yield, 87 %; mp 194 ^{0}C; IR (KBr), υ (cm^{-1}): 3495 (O-H), 3313 (N–H), 2924 (CH_3 str), 2210 (N_3), 1635 (N-H deformation for pri. amine), 548 (C-I str.), 1474 (-CH_3 bend), 1382 (-CH_3 bend.), 1398 (C=N str.), 1526 (C=C bend.), ^{1}H NMR ($CDCl_3$), δ (ppm): 1.9 (s, 3H, -CH_3), 4.8 (s, 2H, -NH_2), 7.1 (s, 1H, Ha), 7.3 (s, 1H, Hb), 7.31-7.41 (m, 5H, Ar-H), 10.1 (s, 1H, -OH). ^{13}C NMR (200 MHz $CDCl_3$), δ 21.70, 47.57, 63.52, 86.22, 86.32, 66.83, 125.87, 127.10, 128.02, 128.55, 129.59, 131.23, 132.56, 134.76, 138.65, 148.92, 152.51, 164.83 Mass (m/z): 444 M^+; Elemental analysis: Calculated for ($C_{17}H_{13}IN_6O$): C, 45.96; H, 2.95; I, 28.57; N, 18.92; O, 3.60 Found: C, 45.90; H, 2.91; I, 28.61; N, 18.98; O, 3.54.

2-(2-amino-5-azido-6-phenylpyrimidin-4-yl)-4-chloro-6-iodophenol (2f)
Yield, 85 %; mp 265 ^{0}C; IR (KBr), υ (cm^{-1}): 3502 (O-H), 3314 (N–H), 2922 (CH_3 str), 2200 (N_3), 1640 (N-H deformation for pri. amine), 546 (C-I str.), 1470 (-CH_3 bend), 1382 (-CH_3 bend.), 1399 (C=N str.), 1531 (C=C bend.), ^{1}H NMR ($CDCl_3$), δ (ppm): 4.0 (s, 2H, -NH_2), 7.41-7.47 (m, 5H, Ar-H), 7.6 (s, 1H, Ha), 7.7 (s, 1H, Hb), 12.4 (s, 1H, -OH). ^{13}C NMR (200 MHz $CDCl_3$), δ 89.77, 99.13, 121.16, 123.79, 126.93, 127.77, 128.35, 129.08, 129.87, 138.99, 158.21, 161.01, 161.83, 162.17 Mass (m/z): 463 M^+; Elemental analysis: Calculated for ($C_{16}H_{10}ClIN_6O$): C, 41.36; H, 2.17; Cl, 7.63; I, 27.31; N, 18.09; O, 3.44 Found: C, 41.32; H, 2.11; Cl, 7.55; I, 27.37; N, 18.12; O, 3.48.

4-(2-amino-5-azido-6-phenylpyrimidin-4-yl) benzene-1,3-diol (2g)
Yield, 72 %; mp 164 ^{0}C; IR (KBr), υ (cm^{-1}): 3554 (O-H), 3316 (N–H), 3122 (CH_3 str), 2180 (N_3), 1636 (N-H deformation for pri. amine), 1474 (-CH_3 bend), 1382 (-CH_3 bend.), 1398 (C=N str.), 1526 (C=C bend.), ^{1}H NMR ($DMSOd_6$), δ (ppm): 5.1 (s, 2H, -NH_2), 6.910 – 6.912 (d, 1H, J = 0.6, Ha), 7.1-7.2 (dd, 1H, J = 4.08, 8.32, Hb), 7.4-8.6 (m, 5H, Ar-H), 8.11-8.12 (d, 1H, J = 6.44, Hc), 12.7 (s, 2H, -OH). ^{13}C NMR (200 MHz $DMSOd_6$), δ 98.99, 105.07, 108.64, 113.91, 126.96, 129.02, 130.05, 132.58, 134.25, 157.28, 158.55, 160.06, 161.12, 162.82 Mass (m/z): 320 M^+; Elemental analysis: Calculated for ($C_{16}H_{12}N_6O_2$): C, 60.00; H, 3.78; N, 26.24; O, 9.99 Found: C, 60.04; H, 3.72; N, 26.28; O, 9.91.

2-(2-amino-5-azido-6-phenylpyrimidin-4-yl)-4-methyl-6-nitrophenol (2h)
Yield, 70 %; mp 210 ^{0}C; IR (KBr), υ (cm^{-1}): 3494 (O-H), 3316 (N–H), 2928 (CH_3 str), 2145 (N_3), 1635 (N-H deformation for pri. amine), 1512 (-NO_2 str.), 1474 (-CH_3 bend), 1384 (-CH_3 bend.), 1397 (C=N str.), 1527 (C=C bend.), ^{1}H NMR ($CDCl_3$), δ (ppm): 2.3 (s, 3H, -CH_3), 5.0 (s, 2H, -NH_2), 6.8 (S, 1H, Ha), 6.84–6.99 (m, 5H, Ar-H), 7.39 (s, 1H, Hb), 10.1 (s, 1H, -OH). ^{13}C NMR (200 MHz $CDCl_3$), δ 20.6, 99.2, 120.9, 126.7, 127.2, 128.1, 128.5, 129.1, 132.3, 136.8, 137.0, 148.1, 158.8, 162.2, 164.0 Mass (m/z): 363 M^+; Elemental analysis: Calculated for ($C_{17}H_{13}N_7O_3$): C, 56.20; H, 3.61; N, 26.99; O, 13.21 Found: C, 56.28; H, 3.56; N, 26.92; O, 13.19.

2-(2-amino-5-azido-6-phenylpyrimidin-4-yl)-4-chloro-6-nitrophenol (2i)
Yield, 76 %; mp 194 ^{0}C; IR (KBr), υ (cm^{-1}): 3504 (O-H), 3315 (N–H), 2923 (CH_3 str), 2156 (N_3), 1635 (N-H deformation for pri. amine), 1514 (-NO_2 str.), 1477 (-CH_3 bend), 1385 (-CH_3 bend.), 1395 (C=N str.), 1527 (C=C bend.), ^{1}H NMR ($CDCl_3$), δ (ppm): 4.4 (s, 2H, -NH_2), 6.57–6.81 (m, 5H, Ar-H), 7.0 (s, 1H, Ha), 7.1 (s, 1H, Hb), 10.5 (s, 1H, -OH). ^{13}C NMR (200 MHz $CDCl_3$), δ 98.49, 123.11, 124.92, 125.59, 127.00, 127.26, 127.76, 128.13, 135.09, 139.06, 149.02, 158.85, 161.20, 164.05 Mass (m/z): 383 M^+; Elemental analysis: Calculated for ($C_{16}H_{10}ClN_7O_3$): C, 50.08; H, 2.63; Cl, 9.24; N, 25.55; O, 12.51 Found: C, 50.01; H, 2.56; Cl, 9.19; N, 25.48; O, 12.45.

5-azido-4-(2,4-dimethoxyphenyl)-6-phenylpyrimidin-2-amine (2j)
Yield, 58 %; mp 110 ^{0}C; IR (KBr), υ (cm^{-1}): 3496 (O-H), 3316 (N–H), 2924 (Ar-CH str.), 2816 (C-H str. CH_3-O-), 2178 (N_3), 1637 (N-H deformation for pri. amine), 1472 (-CH_3 bend), 1384 (-CH_3 bend.), 1397 (C=N str.), 1527 (C=C bend.), ^{1}H NMR ($CDCl_3$), δ (ppm): 3.3 (s, 6H, -OCH_3), 4.8 (s, 2H, -NH_2), 6.8-6.9 (d, 1H, J = 8.36, Ha), 7.10-7.12 (dd, 1H, J = 1.6, 1.64, Hb), 7.34–7.48 (m, 5H, Ar-H), 7.49-7.50 (d, 1H, J = 1.36, Hc). ^{13}C NMR (200 MHz $CDCl_3$), δ 55.83, 56.16, 98.83, 98.91, 107.26, 111.12, 125.16, 127.24, 129.09, 130.63, 134.46, 157.06, 158.49, 160.22, 161.49, 165.80 Mass (m/z): 348 M^+; Elemental analysis: Calculated for ($C_{18}H_{16}N_6O_2$): C, 62.06; H, 4.63; N, 24.12; O, 9.19 Found: C, 62.01; H, 4.66; N, 24.15; O, 9.11.

5-azido-4-(5-bromo-2,4-dimethoxyphenyl)-6-phenylpyrimidin-2-amine (2k)
Yield, 91 %; mp 178 ^{0}C; IR (KBr), υ (cm^{-1}): 3492 (O-H), 3310 (N–H), 2922 (Ar-CH str.), 2814 (C-H str. CH_3-O-), 2122 (N_3), 1635 (N-H deformation for pri. amine), 610 (C-Br str.), 1474 (-CH_3 bend), 1382 (-CH_3 bend.), 1397 (C=N str.), 1530 (C=C bend.), ^{1}H NMR (DMSOd_6), δ (ppm): 3.2 (s, 6H, -OCH_3), 4.1 (s, 2H, -NH_2), 6.92–7.11 (m, 5H, A-rH), 7.21 (s, 1H, Ha), 7.32 (s, 1H, Hb). ^{13}C NMR (200 MHz DMSOd_6), δ 55.12, 55.48, 98.76, 100.82, 104.77, 113.02, 126.03, 127.22, 129.04, 130.61, 136.56, 157.77, 158.48, 159.92, 164.19, 165.63 Mass (m/z): 426 M^+; Elemental analysis: Calculated for ($C_{18}H_{15}BrN_6O_2$): C, 50.60; H, 3.54; Br, 18.70; N, 19.67; O, 7.49 Found: C, 50.56; H, 3.51; Br, 18.69; N, 19.61; O, 7.47.

5-azido-4-(5-iodo-2,4-dimethoxyphenyl)-6-phenylpyrimidin-2-amine (2l)
Yield, 78 %; mp 182 ^{0}C; IR (KBr), υ (cm^{-1}): 3506 (O-H), 3311 (N–H), 2923 (Ar-CH str.), 2818 (C-H str. CH_3-O-), 2146 (N_3), 1641 (N-H deformation for pri. amine), 548 (C-I str.), 1471 (-CH_3 bend), 1385 (-CH_3 bend.), 1391 (C=N str.), 1531 (C=C bend.), ^{1}H NMR (DMSOd_6), δ (ppm): 3.5 (s, 6H, -OCH_3), 4.4 (s, 2H, -NH_2), 7.1 (s, 1H, Ha), 7.2–7.3 (m, 5H, Ar-H), 7.4 (s, 1H, Hb). ^{13}C NMR (200 MHz DMSOd_6), δ 55.07, 55.53, 78.59, 98.96, 100.10, 112.16, 125.24, 127.11, 129.72, 130.62, 138.95, 157.71, 160.22, 163.11, 164.74, 165.69 Mass (m/z): 474 M^+; Elemental analysis: Calculated for ($C_{18}H_{15}IN_6O_2$): C, 45.59; H, 3.19; I, 26.76; N, 17.72; O, 6.75 Found: C, 45.52; H, 3.17; I, 26.79; N, 17.74; O, 6.77.

Docking simulation
1ea1
The file containing the crystal structure of cytochrome P450α-sterol demethylase (14DM) with its selective inhibitor i.e. Fluconazole (470TPF) in the active site (PDB entry 1ea1, six ligand) was downloaded. It is monomer structure with only chain A consisting of 449 residues. This chain A has 470YPF, water and 1 heme (HEM) groups. The chain A with residues, water and the hetero groups (HEM) within a radius of 5 A˚ was refined and cleaned by checking the hybridization, valence of the ligand and introducing H-atoms to the protein residues. 1ea1 carries net charge 2 and 3590 atoms. The asymmetric Unit of 1EA1- cytochrome p450 14 alpha-sterol demethylase (CYP51) from mycobacterium tuberculosis in complex with fluconazole is shown in (**Fig. 3**).

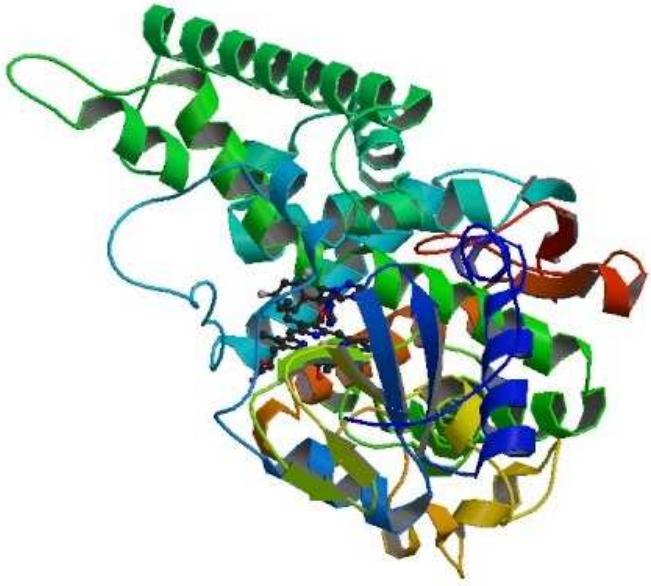

Figure 3 Asymmetric Unit of 1EA1- cytochrome p450 14 alpha-sterol demethylase (CYP51) from mycobacterium tuberculosis in complex with fluconazole

1jij
SB-219383 and its analogues are a class of potent and specific inhibitors of bacterial tyrosyl-tRNA synthetases PDB entry 1jij was selected and used for docking study. As SB-219383 plays the role of inhibitor, the vicinity where this SC 558 is situated should be an active site. Therefore, SB-219383 was taken out from pdb file of this tyrosyl-tRNA synthetases and treated as the so-called model inhibitor for the docking study. The ligand and water molecules were

removed, and all missing hydrogens were added. The asymmetric Unit of 1JIJ - Crystal structure of *S. aureus* TyrRS in complex with SB-239629 is shown in (**Fig. 4**).

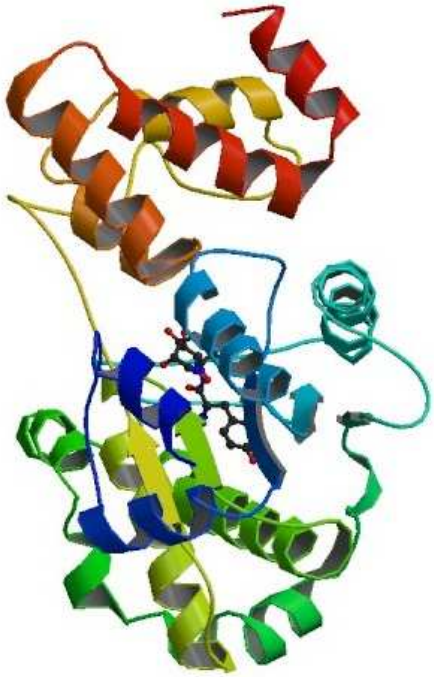

Figure 4 Asymmetric Unit of 1JIJ - Crystal structure of *S. aureus* TyrRS in complex with SB-239629

Docking and binding evaluation

In the automated module of Argus Lab ver. 4.0 work systems (2010) [31] (http://www.arguslab.com), the ligand was docked into the active site of 1EA1 and 1JIJ proteins were downloaded from (http://www.rscb.org/) as PDB files using Argus dock with a fast, simplified potential of mean force (PMF). In Argus Lab, ligand's root node (group of bonded atoms that do not have rotatable bonds) is placed on a search point in the binding site, and a set of diverse and energetically favorable rotations is created. For each rotation, torsions in breadth-first order are constructed, and those poses that survive the torsion search are scored. The N-lowest energy poses are retained, and the final set of poses undergoes coarse minimization, re-clustering and ranking. The first step was the construction of ligands in Chemdraw 3D Ultra 8.047 (2008) [32] (www.cambridgesoft.com) followed by their optimization. The Universal Force Field a molecular mechanics method was used initially for cleaning up structures sketched in the builder, and for refining initial geometries. An empirical scoring function was AScore based on XScore of Wang and coworkers [33]. The docking is carried with flexible ligand into a rigid protein-active site. The general procedure for docking process starts with the addition of energy-minimized target ligand on the enzyme. The active site and the ligand were specified in the program. The different starting parameters were optimized by using 15 X 15 X 15 box located at the center of the target active site using a united atom (explicit hydrogen are not considered) potential of mean force (PMF) with a docking algorithm that has a population of 50 chromosomes and runs for 6,000 generations. The process of docking is repeated until a constant value of docking score is reached. This takes about 12,000–18,000 generations. The final results are parameterized in terms of docking score in kcal/mole, which are depicted in **Tables 6**. The docked ligand–active site complex is interpreted by looking at the H-bonding or hydrophobic interaction of the ligand with the amino acid residues in the active site. The same procedure was followed for docking different substituted azido derivatives of pyrimidines into the active site of 1EA1 and 1JIJ enzymes.

RESULTS AND DISCUSSION

Virtual designing of library of compounds

A library of 25 molecules was designed. The newly tailored molecules were considered as standard templates for docking studies. Overall, amongst 25 virtual molecules as depicted in **Table 1**, 12 molecules displayed the highest

negative binding scores (**2a–l**), and the other 8 (**2m- y**) molecules exhibited negligible results and were thus discarded.

Table 1 List of virtually designed analogues of azido derivatives of pyrimidines

Sr. No.	Compounds 2a-y
1	2-(2-amino-5-azido-6-phenylpyrimidin-4-yl)-4-methylphenol (2a)
2	2-(2-amino-5-azido-6-phenylpyrimidin-4-yl)-4-chlorophenol (2b)
3	2-(2-amino-5-azido-6-phenylpyrimidin-4-yl)-6-bromo-4-methylphenol (2c)
4	2-(2-amino-5-azido-6-phenylpyrimidin-4-yl)-6-bromo-4-chlorophenol (2d)
5	2-(2-amino-5-azido-6-phenylpyrimidin-4-yl)-6-iodo-4-methylphenol (2e)
6	2-(2-amino-5-azido-6-phenylpyrimidin-4-yl)-4-chloro-6-iodophenol (2f)
7	4-(2-amino-5-azido-6-phenylpyrimidin-4-yl)benzene-1,3-diol (2g)
8	2-(2-amino-5-azido-6-phenylpyrimidin-4-yl)-4-methyl-6-nitrophenol (2h)
9	2-(2-amino-5-azido-6-phenylpyrimidin-4-yl)-4-chloro-6-nitrophenol (2i)
10	5-azido-4-(2,4-dimethoxyphenyl)-6-phenylpyrimidin-2-amine (2j)
11	5-azido-4-(5-bromo-2,4-dimethoxyphenyl)-6-phenylpyrimidin-2-amine (2k)
12	5-azido-4-(5-iodo-2,4-dimethoxyphenyl)-6-phenylpyrimidin-2-amine (2l)
13	5-azido-4-(2,4-diethoxyphenyl)-6-phenylpyrimidin-2-amine (2m)
14	5-azido-4-(5-bromo-2,4-diethoxyphenyl)-6-phenylpyrimidin-2-amine (2n)
15	5-azido-4-(3-bromo-5-methylphenyl)-6-phenylpyrimidin-2-amine (2o)
16	5-azido-4-(3-fluoro-5-methylphenyl)-6-phenylpyrimidin-2-amine (2p)
17	5-azido-4-(3-fluorophenyl)-6-phenylpyrimidin-2-amine (2q)
18	5-azido-4-(3-bromo-5-fluorophenyl)-6-phenylpyrimidin-2-amine (2r)
19	5-azido-4-(3-fluoro-5-nitrophenyl)-6-phenylpyrimidin-2-amine (2s)
20	5-azido-4-(3-bromo-5-nitrophenyl)-6-phenylpyrimidin-2-amine (2t)
21	5-azido-4-(3,5-dinitrophenyl)-6-phenylpyrimidin-2-amine (2u)
22	5-azido-4-(3,5-dibromophenyl)-6-phenylpyrimidin-2-amine (2v)
23	5-azido-4-(3-bromo-5-fluorophenyl)-6-phenylpyrimidin-2-amine (2w)
24	5-azido-4-(3-bromo-5-chlorophenyl)-6-phenylpyrimidin-2-amine (2x)
25	5-azido-4-(3-chloro-5-fluorophenyl)-6-phenylpyrimidin-2-amine (2y)

Chemistry

The synthetic route was achieved through ionic liquid [bmim][PF_6] serving as dual solvent and catalyst, leading to quick, easy and enhanced yield. This rational chemical approach afforded azido derivative of pyrimidines.

Substituted azido pyrimidines were synthesized efficiently by cyclization of 3-azido-6-substituted-2-phenyl-4H-chromen-4-one using guanidine carbonate in [bmim][PF_6]. The whole procedure is simple and straightforward. By employing this protocol, a series of novel 2-(2-amino-5-azido-4,5-dihydro-6-phenylpyrimidin-4-yl)-4-substituted phenols hybrids were prepared.

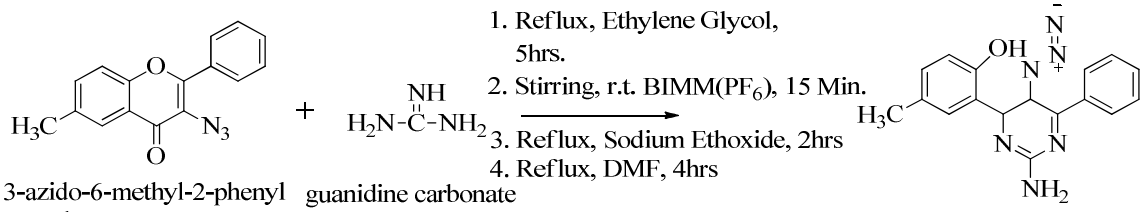

Scheme 1 Synthesis of 2-(2-amino-5-azido-4,5-dihydro-6-phenylpyrimidin-4-yl)-4-methylphenol 2a

The reaction of **1a** in ethylene glycol at reflux was complete within 5 hours, giving **2a** in 80% isolated yield (**Table 2, entry 1**). The reaction time was carefully regulated to avoid the decomposition of the product and the formation of byproducts. The yield of **2a** was drastically reduced using N,N-dimethylformamide at reflux for 4 hours (**entry 3**); the latter reaction resulted in a 65% yield. It was observed that the reaction proceeded well on changing solvent to sodium ethoxide reaction time reduces to 2 hours: the yield improved to 85% (**entry 2**). Thus, the efficiency of the reaction was markedly influenced by the nature of the solvent, i.e. by increasing the hydrophilicity of the reaction mixture, indicating a preference for protic conditions. Additionally, the reactions in the ionic liquids

functions dually as solvent and catalyst. The use of [bmim][PF_6] resulted in much higher reaction rates in 15 min. at room temperature: the yield improved to 97% (**entry 4**) (**Scheme 1**) than those of the reactions performed in common organic solvents (**entries 1–3**).

Table 2 Optimization of the Reaction Conditions for the Synthesis of 2-(2-amino-5-azido-6-phenylpyrimidin-4-yl)-4-methylphenol (2a)

Entry	Solvent	Temperature	Reaction rate	Final isolated yield (%)
1	Ethylene Glycol	reflux	5hrs	80
2	DMF	reflux	4hrs	65
3	Sodium Ethoxide	reflux	2hrs	85
4	[bmim][PF_6]	r.t.	15 min	97

The effectiveness of ionic liquid continued unaffected even after its recycle and frequent use up to ten times; however, there was a noticeable drop in yield after the 10^{th} cycle, suggesting that the catalyst may have become contaminated, degraded, or exhausted (**Table 3**). The preferred product appeared in homogeneous phase and was isolated by adding water to reaction mix. Ionic liquid was found to be soluble in water and crude product was separated which was further recrystallized by ethanol. After each cycle, the product was isolated and the water which was left in ionic liquid was removed under vacuum and oven dried to reuse the ionic liquid for subsequent cycle. The conversion level was found to be declined after its tenth cycle. Our protocol has a merit of being environmentally benign and a simple operation, involving convenient workup, a short reaction time, and proceeding in good to excellent yields.

Table 3 Effect of reuse of [bmim][PF_6] ionic liquid on the formation of 2a

Entry	Recycling	Isolated yield (%)
1	0	97
2	1	95
3	2	92
4	3	92
5	4	90
6	5	90
7	6	89
8	7	89
9	8	85
10	9	85
11	10	85
12	11	70
13	12	56

The structure of 2-(2-amino-5-azido-6-phenylpyrimidin-4-yl)-4-methylphenol **2a** was supported by elemental analysis, IR, ^{1}HNMR, ^{13}CNMR, and MASS spectral data. IR spectra exhibited an O–H absorption band at 3498 cm^{-1}, Primary amine group at 3312 cm^{-1}, azide group at 2138 cm^{-1}, -CH_3 stretch at 2922 cm^{-1}, C,N stretch at 1395 cm^{-1}. ^{1}HNMR ($CDCl_3$/$DMSOd_6$) was nicely resolved and showed the appearance of –CH_3 protons as siglet at δ 2.3, also, -NH_2 proton as a characteristic singlet at δ 4.6 and the aromatic protons as a multiplet at δ 6.91– 8.1. The appearance of siglet of 1 proton at δ 13.6 showed the presence of hydroxyl group attached to the basic moiety; the appearance of the –NH_2 peak at δ 4.6 confirmed the formation of product **2a**. ^{13}CNMR, MASS spectral analysis and elemental analysis also support the formation of product **2a**. The general structure of compounds **2a-l** is depicted in **figure 5**, physical data of newly synthesized compounds **2a-l** is tabulated in **Table 4**.

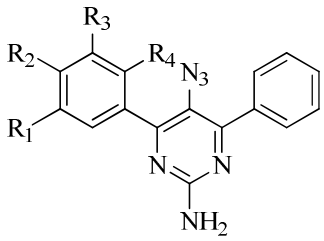

Figure 5 General structure of compounds 2a-l

Table 4 Physical data of newly synthesized compounds 2a-l

Entry	Comp.	MF	R_1	R_2	R_3	R_4	MW	MP in ^{0}C	Yield in %	
									Conventional	Ionic liq.
1	2a	$C_{17}H_{16}N_6O$	CH_3	H	H	OH	318	210	80	97
2	2b	$C_{16}H_{13}ClN_6O$	Cl	H	H	OH	338	244	73	95
3	2c	$C_{17}H_{15}BrN_6O$	CH_3	H	Br	OH	396	188	67	90
4	2d	$C_{16}H_{12}BrClN_6O$	Cl	H	Br	OH	417	256	69	94
5	2e	$C_{17}H_{15}IN_6O$	CH_3	H	I	OH	444	194	56	87
6	2f	$C_{16}H_{12}ClIN_6O$	Cl	H	I	OH	463	265	51	85
7	2g	$C_{16}H_{14}N_6O_2$	H	OH	H	OH	320	164	64	72
8	2h	$C_{17}H_{15}N_7O_3$	CH_3	H	NO_2	OH	363	210	56	70
9	2i	$C_{16}H_{12}ClN_7O_3$	Cl	H	NO_2	OH	383	194	62	76
10	2j	$C_{18}H_{18}N_6O_2$	H	OCH_3	H	OCH_3	348	110	48	58
11	2k	$C_{18}H_{17}BrN_6O_2$	Br	OCH_3	H	OCH_3	426	178	67	91
12	2l	$C_{18}H_{17}IN_6O_2$	I	OCH_3	H	OCH_3	474	182	54	78

X-ray powder diffraction analysis

Single crystals of compound **2a** could not be obtained; hence XRD patterns of the same were studied. All compounds were found to be crystalline and their X-ray powder diffractograms were collected. The lattice parameters and Miller indices were computed. The indexing and calculation of unit cell parameters are performed with the help of Powder -X Software. The calculated and observed 2θ value, the relative intensity, inter-planar distance along with Miller's indices for corresponding angles are tabulated for the compound. On the basis of X-ray powder patterns and unit cell refinements, it is found that the compound **2a** adopt monoclinic crystal system with C*/c type of lattice space group. The lattice constants calculated are depicted in **Table 5**. **Figure 6** shows the ORTEP drawing of the molecule **2a** showing the atomic numbering system.

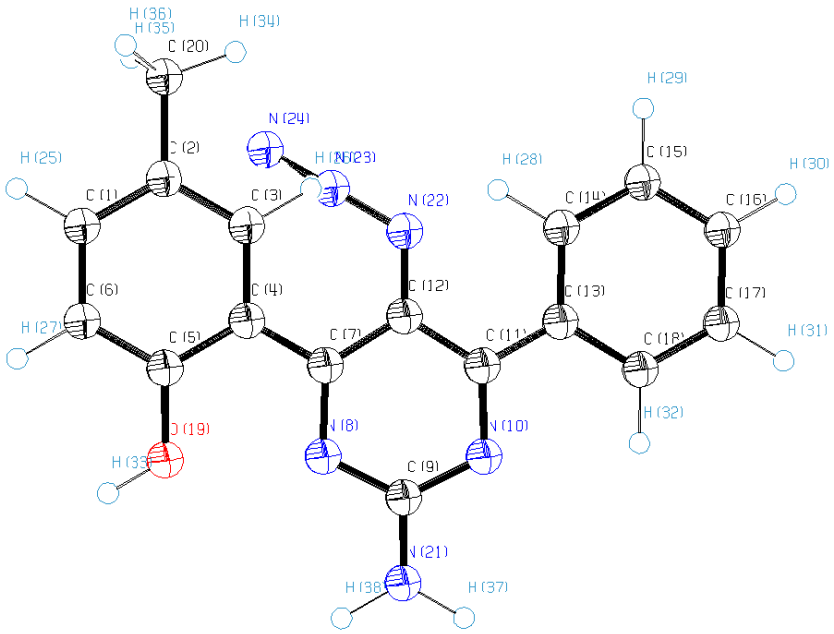

Figure 6 An ORTEP [34] drawing of the molecule 2a showing the atomic numbering system

Table 5 Powder XRD data of 2-(2-amino-5-azido-6-phenylpyrimidin-4-yl)-4-methylphenol

Data	2-(2-amino-5-azido-6-phenylpyrimidin-4-yl)-4-methylphenol
Chemical formula	$C_{17}H_{16}N_6O$
Molecular weight (g/mol)	320.35
Crystal system	Monoclinic
Space group	C*/c
Space group number:	15
Unit cell dimensions:	
a	30.3
b	8.47
c	20.78
α	90
β	127.8
γ	90
Volume	4213.9
(Cal.) Density (g/cm^{-3})	1.65
Z	8
Temperature	299 K

Computational simulation of antibacterial and antifungal

Docking is a term used for computational schemes that attempt to find the "best" matching between two molecules: a receptor and a ligand. The simulation of newly synthesized compounds as antibacterial and antifungal agents using the molecular modeling tool of protein- ligand interaction to predict the drug structure activity relationship was carried out. Azido analogues of pyrimidine have displayed more binding energies as compared to standard drugs, revealing the fact that these compounds can be promising candidates as antibacterial and antifungal agents.

The potent activity of synthesized compounds (**2a-l**) as new antimicrobial agents, prompted us to study the docking of these derivatives inside the active site of Cyp51 of *C. albicans* and *S. aureus* TyrRS, the potential target for anti-fungal and antibacterial agents respectively. To visualize the interaction of designed scaffold with Cyp51 of *C. albicans* and *S. aureus* TyrRS, docking studies were carried out. All the synthesized azido pyrimidine molecules show binding in the active site of P450 (14DM) CPY51 and *S. aureus* TyrRS active site with binding score between -7.22 and -9.99 kcal/mol (**Table 6**). Compounds 2c, 2d, 2h, 2i show the highest binding with P450 (14DM) in comparison to selective drug i.e. Fluconazole, and compound **2h** shows highest binding with tyrosyl-tRNA synthetases in comparison to selective drug i.e. Ampicillin. Further rationalization of modes of P450 (14DM) CPY51 and *S. aureus* TyrRS active site has been based upon the amino acid residues present around the ligand, in the active site pocket of 1ea1and 1jij. On the basis of structural features essential for binding in the cavity, the azido pyrimidine molecules could be divided into three segments: Substituted Phenyl ring, Central pyrimidine ring with azido group, Phenyl ring. The residues surrounding each Substituted Phenyl ring, Central pyrimidine ring with azido group and Phenyl ring molecules have been determined (**Table 7**).

2-(2-amino-5-azido-6-phenylpyrimidin-4-yl)-4-methyl-6-nitrophenol (**2h**) binds in the active site of cytochrome P450 (1ea1) mainly through hydrophobic interaction. 2-(2-amino-5-azido-6-phenylpyrimidin-4-yl)-4-methyl-6-nitrophenol (**2h**) mainly has two phenyl ring attached to the pyrimidine ring. Phenyl ring (C) is surrounded by TYR76, LEU321 and PHE78; Central pyrimidine ring with azido group (B) is enveloped by MET79, THR260 and PHE255 (**Fig. 7a-b**). It also contains one Nitro-substituted phenyl ring (A) which approaches LEU100, ARG96 and ALA256. Therefore $–NO_2$ substituted phenyl ring present on 2-(2-amino-5-azido-6-phenylpyrimidin-4-yl)-4-methyl-6-nitrophenol (**2h**) through p–p interaction with amino acid residues kept in place in active site of cytochrome P450, increases the binding energy, by -9.46 kcal/mol (**Table 6**).

Within vitro activity against tyrosyl-tRNA synthetase from *S. aureus* in hand, it is thought worth-while to do molecular docking studies to support the potency of inhibition. To this end, molecular docking of the most potent inhibitor **2a-1** into SB-239629 binding site of tyrosyl-tRNA synthetase was performed on the binding model based on the tyrosyl-tRNA synthetase complex structure (1jij.pdb) [5]. The interactions between compound **2a-1** and the active site residues of tyrosyl-tRNA synthetase are shown in **Fig. 8a-b**.

Compound **2h** which exhibited the most Binding energy have docked in the vicinity of hydrophobic pocket of MET79, PHE255, LEU100, ARG96, ALA256, THR260, TYR76, LEU321, PHE78 and PHE54, ASP80, ASP40, HIS50, GLY38, PRO53, ASP195, GLY193, HIS50 amino acid residues of P450 (14DM) and S. aureus TyrRS

respectively are shown in **Fig. 7a-b** and **Fig. 8a-b**. Azido moiety is at the entry gate of charged amino acid residues that is MET79 and PHE54.

Three week hydrogen-bonding interactions together with some hydrophobic interactions anchoring **2h** to the active site tightly may explain its excellent inhibitory activity. In brief, the pyrimidine-ring system in the side chain of **2h** occupies the SB-239629 piperidyl-binding pocket, and was oriented towards the entrance cavity (**Fig. 7a-b** and **Fig. 8a-b**) surrounded by LEU100, ARG96, MET79, LEU321, PHE255 and ALA256. The N atom of pyrimidine-ring as a hydrogen bond acceptor is hydrogen-bonded to the backbone nitrogen of 96 with H-O bond length of 2.447 Å (**Fig. 7a-b**). Obviously, the pyrimidine-ring system was located at a hydrophilic pocket of the active site. Thus, the most prominent binding is observed in ligands **2a, 2b, 2c** and **2d** as compared to other substituent the pyrimidine ring with P450 (14DM) is surrounded by the hydrophobic pocket of TYR76, PHE78, LEU321, THR260, ALA256, LEU100, and Azido moiety is at the entry gate of charged amino acid residues MET79, PHE255: the docking score is -9.55, -9.55, -9.99k, -9.95cal/mole respectively. For compound **2i, 2j** and **2k** pyrimidine ring approaches in the hydrophobic pocket of S. aureus TyrRS through GLY 193, GLN 196, GLN 190, GLN 174, TYR 36, LEU 70 ASN 124, GLY 38, PRO 53, PHE 54, HIS 50 the azido moiety attached to pyrimidine nucleus is surrounded by ASP 80, TYR 170: the docking score is -8.18, -8.73, -8.51 kcal/mole respectively.

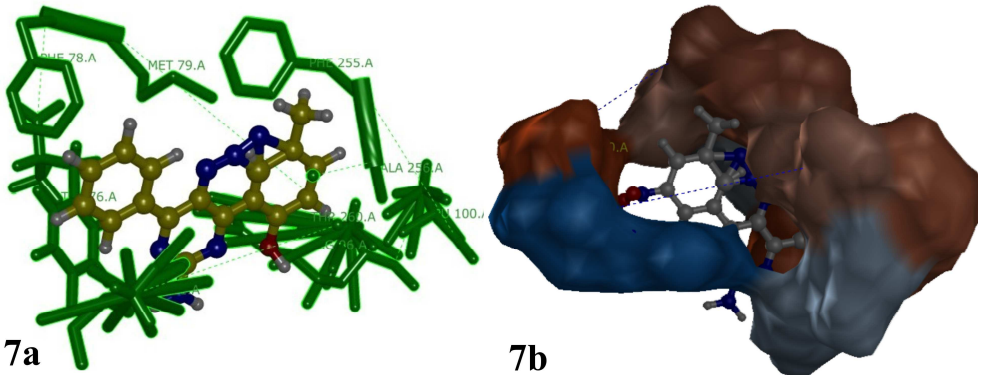

Figure 7a-b Binding mode of compound 2h with P450 (14DM) CPY51. The enzyme is shown as surface; while 2h docked structure is shown as ball and sticks. This figure was made using Chimera

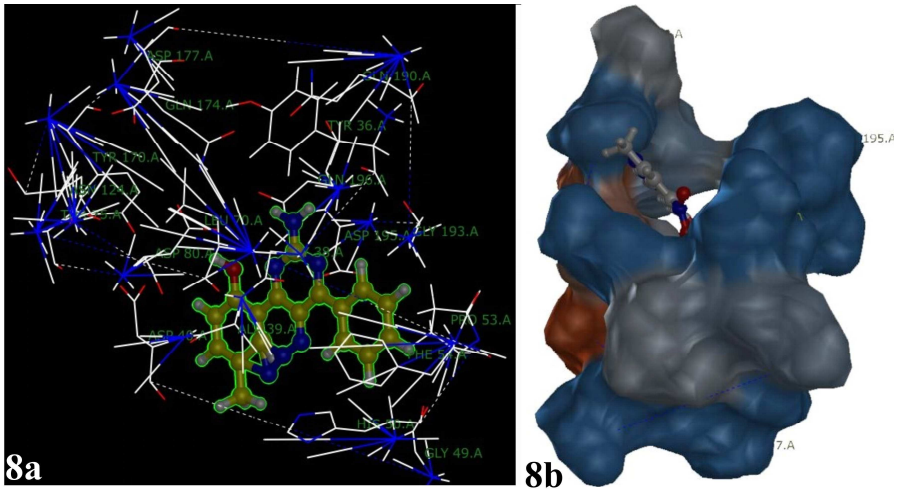

Figure 8a-b Binding mode of compound 2h with TyrRS. The enzyme is shown as surface; while 2h docked structure is shown as ball and sticks. This figure was made using Chimera

Table 6 Binding energies (Kcal/mole) of Pyrimidine analogues 2a-l and standard drugs with protein (pdb entry: 1EA1 and 1JIJ)

Sr. No.	Ligand	Binding Energy (Kcal/mol)1EA1	Binding Energy (Kcal/mol) 1JIJ
1	2a	-9.55	-8.95
2	2b	-9.55	-7.54
3	2c	-9.99	-7.22
4	2d	-9.95	-8.02
5	2e	-	-
6	2f	-	-
7	2g	-8.84	-7.64
8	2h	-9.46	-9.19
9	2i	-9.27	-8.18
10	2j	-8.98	-8.73
11	2k	-9.37	-8.51
12	2l	-	-
13	Standard	-8.11 (Fluconazole)	-9.13 (Ampicillin)

Table 7 Amino acid residues around all segment of azido derivatives of pyrimidines (2a–l) docked with 1EA1 and 1JIJ active site

Sr. No.	Ligand	1EA1			1JIJ		
		Substituted Phenyl ring	Central pyrimidine ring with azido group	Phenyl ring	Substituted Phenyl ring	Central pyrimidine ring with azido group	Phenyl ring
1	2a	PHE255, ARG96, LEU100, ALA256	LEU321, THR260	MET79, TYR76, LEU321, PHE78	GLN196, ASP195, GLY193, ASP80	ALA39, GLY38, ASP40, LEU70	PRO53, PHE54, HIS50, GLY49
2	2b	ARG96, LEU100, ALA256	LEU321, PHE255, THR260	MET79, TYR76, PHE78	PRO53, GLY49, GLY193, GLN196	PHE54, GLY193, HIS50	ASP80, GLN90, GLY38, TYR36, LEU70
3	2c	THR260, LEU321, PHE78	PHE255, TYR96, ALA256,	LEU100, ARG96, MET79,	PHE54, HIS50, GLY38, ASN124	PRO53, ALA39, ASP40, THR75	GLY193, ASP195, GLN196, ASP80
4	2d	ARG96, LEU100, ALA256	PHE255, THR260	PHE78, TYR76, MET79, LEU321	TYR36, PRO53, ASP40, GLY193	ALA39, GLN190, PHE54	LEU70, THR75, ASN124
5	2g	ALA256, ARG96, LEU100	MET79, THR260, PHE255	PHE78, LEU321, TYR76	GLY193, ASP195, GLY49, HIS50, PRO53	ASP80, ALA39, ASP40, PHE54	THR75, LEU70, TYR36
6	2h	LEU100, ARG96, ALA256	MET79, THR260, PHE255	TYR76, LEU321, PHE78	ALA39, LEU70, ASP40	PHE54, ASP80, HIS50, GLY38	PRO53, ASP195, GLY193, HIS50
7	2i	ARG96, ALA256, LEU100	THR260, LEU321, PHE255	TYR76, PHE78, MET79, THR260	LEU70, THR75, TYR170, ASP177	HIS50, GLY193, PRO53	ASP40, ALA39, PHE54, GLY38
8	2j	ALA256, LEU100, ARG96	THR260, PHE255, MET79	LEU321, TYR76, PHE78	GLY193, GLN196, GLY49, TYR170	ASP80, GLY38, PHE54, TYR36	PRO53, ASP195, HIS50
9	2k	LEU100, ARG96	ALA256, TYR76, PHE255	THR260, LEU321, PHE78	PRO53, ASP195, GLY193, GLN196	TYR170, ASP80, ALA39, ASP40	THR75, TYR36, LEU70, ASN124, GLY38

***In vitro* anti-bacterial and anti-fungal activity:**

All azidopyrimidine derivatives are screened against Gram –ve bacteria [*Salmonella typhi* (ATCC 23564)] Gram +ve bacteria [*Staphylococcus aureus* (ATCC 1538P)] and *C. albicans* (ATCC 2091); *Aspergillus Niger* (ATCC 16880) as antifungal agents. The cytotoxicity of all scaffolds was compared with Ampicillin for antibacterial study and Fluconazole for antifungal study. The antimicrobial screening was carried out by cup-plate method [35] at

concentration of 100 ug/mL in solvent DMSO. The test compounds under investigation were incorporated into agar, which had previously been inoculated with the test organisms.

The results were compared with Ampicillin and Fluconazole as standard drugs. The inoculated plates were incubated at 37^0C for 24 hours in case of bacteria and 48 hours in case of fungus. The zone of inhibition was expressed in mm and compared with the standard drugs. **Table 8** shows the Antimicrobial-screening results of synthesized compounds **2a–l**.

Table 8 Antimicrobial-screening results of synthesized compounds 2a–l.

Sr. No	Compound No.	Diameter of Zone of inhibition in mm.			
		S. aureus	*S. typhi*	*C. albicans*	*A. niger*
1	2a	Absent	10	10	Absent
2	2b	11	10	Absent	Absent
3	2c	12	10	30	16
4	2d	14	11	32	14
5	2e	21	17	12	12
6	2f	23	18	14	14
7	2g	14	14	Absent	Absent
8	2h	19	20	30	12
9	2i	18	15	30	14
10	2j	11	10	30	10
11	2k	12	12	10	Absent
12	2l	23	12	10	10
13	Std.	17	24	37	17
14	DMSO	Absent	Absent	Absent	Absent

Structure–activity relationship

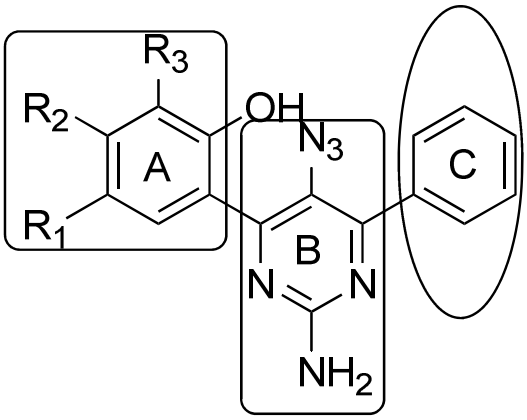

Figure 9 Structure–activity relationships

Structure–activity relationship is the relationship between the chemical and three-dimensional structures of a molecule and its biological activity. The analysis of SAR enables the determination of the chemical groups responsible for evoking a target biological effect in the organism. This allows modification of the effect or the potency of a bioactive compound (typically a drug) by changing its chemical structure. Medicinal chemists insert new chemical groups into the biomedical compound and test the modifications for their biological effects. Our hybrid molecule may be considered as a template scaffold in which one can insert substituent at different positions to enhance the specificity towards microorganisms as pharmacological activities.

It is interesting to note that the compounds **2c, 2d, 2h** and **2i** exhibit significant antifungal activity revealing that the presence of electron withdrawing groups like –Br, -NO_2 as substituent at different position on aromatic ring A (**Fig. 9**) improved the efficacy of the compounds, compound **2h** also exhibited the significant antibacterial activity due to the presence of electron withdrawing –NO_2 group attached to substituted aromatic ring A. The two phenyl rings are essential for modulation of the hydrophobic interaction which enhanced its antifungal activity. Other compounds,

exhibited moderate activity against fungi and bacteria due to the presence of $–OCH_3$ and –OH group on substituted aromatic ring.

Computational details

The simulation of newly synthesized compounds as anti-bacterial and anti-fungal agents using the molecular modeling tool of protein- ligand interaction to predict the drug structure activity relationship was carried out.
A comparative analysis of antimetabolite drug and corresponding metabolites (synthesized compounds) gives a better understanding for rational drug designing. 1EA1 and 1JIJ enzymes docked with novel receptors responded for binding energies.

The pdb files containing the crystal structures of protein (PDB ENTRY 1EA1, 1JIJ) with selective inhibitors were downloaded from protein data bank (http://www.rscb.org/) as PDB files.

The first step was the construction of ligands in Chemdraw 3D Ultra 8.047 followed with their optimization. Argus Lab 4.0484 was used to perform protein ligand interactions study.

The Computational protocol was subjected to all newly synthesized compounds of 2-(2-amino-5-azido-4, 5-dihydro-phenylpyrimidin-4-yl) -4-substituted phenols (**2a-l**) to predict their inhibitory mechanism and selectivity towards 1EA1 and 1JIJ enzymes.

Validation of computational programme

To validate the programme the selective inhibitor as internal ligand was redocked and its docking position was compared with the initial position by root mean square deviation value (RMSD). 470 TPF (inhibitor) for 1EA1, were redocked having RMSD to be 0.442. The close overlapping of ligands ensures the validity of programme, as revealed in **Fig. 10**.

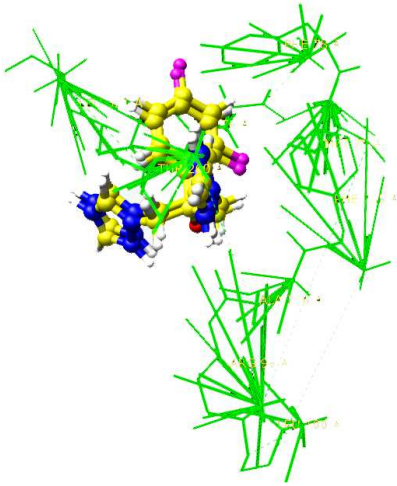

Figure 10 Close overlapping of 470 TPF (inhibitor) for 1EA1 in vicinity of amino acid residue

CONCLUSION

[bmim][PF_6] proved to be an exceptionally efficient dual solvent catalyst system for the synthesis of azido-pyrimidine hybrids at ambient temperature within 15mins. The protocol has the merit of being environmentally friendly and a simple operation, involving convenient workup, a short reaction time, and resulting in good to excellent yields.

Twelve derivatives of 2-(2-amino-5-azido-4,5-dihydro-6-phenylpyrimidin-4-yl)-4-substituted phenols were prepared and tested for their anti-microbial activity. Compound **2h**, 2-(2-amino-5-azido-6-phenylpyrimidin-4-yl)-4-methyl-6-nitrophenol, showed the most potent inhibitory activity with zone of inhibition 19 against *S. aureus*, 20 against *S. typhi*, 30 against *C. albicans* and 12 against *A. niger* (**Table 8**). Substitution with nitro group significantly increased the activity. Molecular dockings of the most potent compound **2h** into P450 (14DM) CPY51 and *S. aureus* TyrRS active site were performed. Many interactions, anchoring the ligand to the active site of the enzyme tightly might

explain its excellent inhibitory activity. This indicates that **2h** would be a potential antimicrobial agent for further research.

Acknowledgments
Authors are thankful to the SAIF, Chandigarh for ^{1}HNMR and ^{13}CNMR spectral analysis, Indian institute of technology Chennai for CNH and Mass spectral analysis and Indian institute of chemical technology Hyderabad for Mass spectral analysis. V.N.I.T. Nagpur for X-ray diffraction data, we are also thankful to Department of Pharmacy, Nagpur for IR spectral analysis. The author also thanks the Director, Institute of Science, Nagpur for providing laboratory facilities. Special Thanks to UGC (UGC Major Project: 37-497/2009 [SR]), New Delhi for financial assistance.

REFERENCES

[1] JH Mohammed; AI Mohammed; SJ Abass, *Journal of Chemistry and Chemical Sciences*, **2015**, 5(6), 317-324.
[2] HW Boucher; GH Talbot; JS Bradley; JE Edwards Jr.; D Gilbert; LB Rice; M Scheld; B Spellberg; J Bartlett, *Clin. Infect. Dis.*, **2009**, 48, 1-12.
[3] JJ Barker, *Drug Discov. Today*, **2006**, 11, 391-404.
[4] I Masip; E Pérez-Payá; A Messeguer, *Comb. Chem. High T. Scr*., **2005**, 8, 235-239.
[5] X Qiu; CA Janson; WW Smith; SM Green; P McDevitt; K Johanson; P Carter; M Hibbs; C Lewis; A Chalker; A Fosberry; J Lalonde; J Berge; P Brown; CS Houge-Frydrych; RL Jarvest, *Protein Sci.*, **2001**, 10, 2008-2016.
[6] AL Stefanska; NJ Coates; LM Mensah; AJ Pope; SJ Ready; SR Warr, *J. Antibiot*., **2000**, 53, 345-350.
[7] R Farhanullah; T Kang; EJ Yoon; EC Choi; S Kim; J Lee, *Eur. J. Med. Chem*., **2009**, 44, 239-250.
[8] P Van de Vijver; GHM Vondenhoff; TS Kazakov; E Semenova; K Kuznedelov; A Metlitskaya; A Van Aerschot; K Severinov, *J. Bacteriol*., **2009**, 191, 6273-6280.
[9] ZP Xiao et al, *European Journal of Medicinal Chemistry*, **2011**, 46, 4904-4914.
[10] A Coates; Y Hu; R Bax; C Page, *Nature Reviews Drug Discovery*, **2002**, 1, 895-910.
[11] SM Hashemi; H Badali; H Irannejad; M Shokrzadeh; S Emami, *Bioorganic & Medicinal Chemistry*, **2015**, 23, 1481–1491.
[12] L Tamas; K Bela, *Mini-Rev. Med. Chem*., **2007**, 7, 900.
[13] BH Vanden; L Koymans; H Moereels, *Pharmacol. Ther*., **1995**, 67, 9.
[14] Y Zheng; A Oehlschlager; N Georgopapadakou; P Hart-man; P Schelige, *J. Am. Chem. Soc*., **1995**, 117, 670.
[15] NB Pathan; AM Rahatgaonkar, *Arabian Journal of Chemistry*, **2011**, doi:10.1016/j.arabjc.**2011**.02.01.
[16] AH Banday; SA Shameem; BA Ganai, *Organic and Medicinal Chemistry Letters*, **2012**, 2, 13.
[17] MG Bhovi; GS Gadaginamath, *Indian Journal of Chemistry*, **2005**, 44B, 1068-1073.
[18] RF Schinazi; MS Chen; WH Prusoff, *J. Med. Chem.*, **1979**, 22(10), 1273–1277.
[19] AE Rashad; OA Heikal; AOH El-Nezhawy; FME Abdel-Megeid, *Heteroatom Chemistry*, **2005**, 16(3).
[20] O Moukha-chafiq et al, *I L Farmaco*, **2002**, 57, 27–32.
[21] RJ Griffin; MA Meek; CH Schwalbe; MFG Stevens, *J. Med. Chem*., **1989**, 32(11), 2468–2474.
[22] AE Rashad; MS Mohamed; MEA Zaki; SS Fatahala, *Arch. Pharm. Chem. Life Sci*., **2006**, 339, 664 – 669.
[23] MSS Palanki; PE Erdman; AM Manning; A Ow; LJ Ransone; C Spooner; C Suto; M Suto, *Bioorg. Med. Chem. Lett*., **2000**, 10, 1645-1648.
[24] MY Jang; SD Jonghe; K Segers; J Anné; P Herdewijn, *Bioorg. Med. Chem*., **2011,** 19, 702–714.
[25] AA Arutyunyan; SS Mamyan; HM Stepanyan; RV Paronikyan, *Pharmaceutical Chemistry Journal*, **2013**, 47(6).
[26] TN Bansode; RM Ansari; YK Gawale, *Pharmaceutical Chemistry Journal*, **2011,** 45(6).
[27] ZP Xiao; XB He; ZY Peng; TJ Xiong; J Peng; LH Chen; HL Zhu, *Bioorg. Med. Chem*., **2011**, 19, 1571.
[28] AA Chaugule; AH Tamboli; FA Sheikh; WJ Chung; H Kim, *Journal of Molecular Liquids*, **2015**, 208, 314–321.
[29] S Manthiriyappan; CK Lee, *J. Mol. Catal. B: Enzym*., **2009**, 60, 1.
[30] C Dong, *J. Appl. Cryst*., **1999**, 32, 838.
[31] Argus Lab 4.0.1 docking software (**2010**). http://www.arguslab.com Accessed June **2012**.
[32] Chemdraw 3D Pro software (**2010**) www.cambridgesoft.com Accessed June **2012**.
[33] Wang Renxiao, Fang Xueliang, Yipin Lu, *J. Med. Chem.*, **2004**, 47:2977–2980.
[34] LJ Farrugia, *J. Appl. Cryst*., **2012**, 45, 849-854.
[35] (a) Barry, A. L., in Illus (Ed), *Antimicrobial Susceptibility Test: Principal and Practices*, Lea and Febiger, Philadelphia, Pa, U.S.A., **1976**, 180; (b) *Biol. Abstr*., **1977**, 64, 25183.